Journal of Sound and Vibration (2002) **256**(3), 475–498
doi:10.1006/jsvi.5001, available online at http://www.idealibrary.com on IDEAL®

EXPERIMENTAL STUDY OF NOISE PRODUCED BY STEADY FLOW THROUGH A SIMULATED VASCULAR STENOSIS

A. O. Borisyuk

Institute of Hydromechanics, Zhelyabova Street 8/4, 03680 *Kiev*-180 *MSP, Ukraine.*
E-mail: oibor@nas.gov.ua

(*Received* 6 *March* 2000, *and in final form* 7 *August* 2001)

An *in vitro* experiment is carried out in order to study the acoustic effects of a vascular constriction (stenosis) in people and provide correlations between these effects and parameters relevant to the hydrodynamic and acoustic processes. For this purpose, we measure the sound produced when water flows through an elastic tube which is either unobstructed or contains a rigid axisymmetric constriction. The sound is measured at the outside of a large annular container filled with water and bounded at the inside by the coaxial elastic tube. The analysis of the acoustic fields shows that a stenosis has *two basic* acoustic effects. These are a general increase in the sound level and the production of a number of additional distinct peaks (new frequency components) in the acoustic power spectrum. The frequencies of these peaks are close to the characteristic frequencies of vortex formation in the disturbed flow region behind a stenosis and the resonance frequencies of vibration of the post-stenotic segment of the tube. Another important result is that the stenosis generated acoustic power is approximately proportional to the fourth power of the stenosis severity and the same power of the flow Reynolds number.

1. INTRODUCTION

In recent times there has been an increase in the number of investigations into the hydrodynamic and associated acoustic fields in situations similar to those which might be encountered in human blood passages and airways. Motivation for this work centres around the hope of developing non-invasive diagnostic techniques capable of deducing the vessel state and finding a stenosis, if present, from an analysis of the sound field recorded periodically from a given patient. Such techniques, to be quantitative, require the availability of exact and complete information about the fundamental mechanisms of vascular sound generation and transmission, as well as the various factors which specify them. These include the rheological properties of the fluid and the character and structure of the flow in the vessel, the physical and geometrical characteristics of the relevant vascular district and stenotic obstruction, the structure and acoustic properties of the human body tissue, etc. With these known, the relationships between the characteristics of the sound source and the recorded acoustic signal can be correctly predicted and further used for solving the inverse problem (namely, locating pathology by changes in the noise field heard at the body surface).

Analysis of the scientific literature shows that the basic properties of flow in pipes with stenoses of the simplest shapes have been investigated in some detail. The investigations of

0022-460X/02/$35.00

Back and Roschke [1], Cassanova and Giddens [2], and the researchers mentioned in the reviews of Young [3] and Mirolyubov [4], have revealed the jet-like structure of the flow beyond axisymmetric expansions in pipes, and the presence of both laminar and turbulent shear layer regimes at the boundary of the jet and the recirculation region located between the stenosis and the point of jet reattachment. Data on jet reattachment length are available in the work of Back and Roschke [1], Young [3], Mirolyubov [4], Clark [5, 6] and Tobin and Chang [7].

Cassanova and Giddens [2] and Crow and Champagne [8] found that the flow downstream of both sharp-edged and contoured axisymmetric stenoses consists of axisymmetric vortex rings. Pedrizzetti [9] has shown the existence of large-scale eddies behind axisymmetric stenosis in the plane of axial symmetry of vessel. Similar results are also available in references [3, 4, 10].

Studies of wall pressure fluctuations and velocity fields downstream of stenoses in rigid [3–6,10–13] and elastic [3, 4, 7, 14, 15] tubes have revealed that the boundary zone of maximum pressure fluctuations caused by the expanding stream occurs at a short distance upstream from the end of the region of separation, within the first two to three diameters of the expansion chamber. The centreline velocity remains equal to the velocity within the obstruction for the first few tube diameters beyond the obstruction and then falls off rapidly, together with the wall pressure. The correlation and spectral characteristics of wall pressure fluctuations in the separated flow region were shown to be similar to the corresponding characteristics of wall pressure in fully developed turbulent pipe flow. Analytical expressions for the wall pressure power spectrum have also been obtained, and the relevant scaling laws derived.

Abdallah and Hwang [10] and Borisyuk [16] found isolated peaks in the power spectrum of turbulent wall pressure behind a constriction and showed that their position in the spectrum depends on the axial distance downstream from the constriction. The frequencies of these peaks were attributed to the characteristic frequencies of large-scale turbulent eddies behind the constriction exit.

The dominant contribution of large-scale turbulent vortex structures to the low-frequency domain of the wall pressure power spectrum was predicted in references [17–19]. This domain was also shown in references [17–19] to dominate the acoustic fields produced by turbulence-excited elastic elements. Small-scale eddies contribute mainly to the high-frequency domain of the spectrum and consequently, to the high-frequency domain of the acoustic power spectrum, which is usually dominated by background noise.

Noise generation by a vessel excited by inner turbulent flow and noise transmission in the body was investigated by Vovk *et al.* [20, 21], Wang *et al.* [22] and Borisyuk [23, 24]. In the frameworks of the acoustic models developed by these authors, relationships between the spectral and correlation characteristics of the acoustic field heard at the body surface and the parameters of the vessel and the turbulent flow were derived, and the transfer function of the thorax was obtained. Using available low-Mach number turbulent wall pressure models [17, 18], the changes in the acoustic field due to changes in the parameters of vessel and mean flow were found. In particular, the noise level was shown in references [23, 24] to increase as the vessel diameter decreases and/or the mean flow velocity increases. The spectral content of the acoustic field was studied only qualitatively.

To the author's knowledge, noise generation by a stenosed vessel into the body has not yet been studied. An attempt to investigate one aspect of this problem is made in this paper. Here an *in vitro* experiment is carried out in order to study the acoustic effects of a vascular stenosis and provide correlation between these effects and parameters relevant to the hydrodynamic and acoustic processes. The paper consists of six sections, a list of literature and an Appendix. A description of the experimental system developed and the hypotheses

used is given in section 2. Section 3 presents the main results obtained, which are then analyzed in section 4. The practical importance of the results is discussed in section 5. The conclusions of the investigation are formulated in section 6, and a list of notations is given in Appendix A.

2. EXPERIMENT

Precise modelling of vascular sound generation and transmission in the body is difficult. However, noting that the characteristic scales and dimensions of the basic factors which specify these two mechanisms are small compared with the acoustic wavelengths of interest in vascular stenosis murmurs, it is possible to make simplifying assumptions. Under these assumptions, the basic elements of the mechanism of generation and transmission of noise can be simulated quite well within the accepted limits of accuracy. As a result, the spectral and correlation characteristics of noise fields measured in an *in vitro* study will be similar to those recorded from patients.

Taking these arguments into account, a suitable experimental system has been developed. A schematic of the test section and its location within the system is shown in Figure 1. Here the basic elements are:

(1) silicone elastic pipes, of inner diameter, D, 16 mm and wall thickness, h, 2 mm ($h/D = 0{\cdot}125$), modelling a larger human blood vessel;
(2) a set of hollow rigid-walled abrupt axisymmetric cylinders, of varying inner diameter, d, and length, l, which represent stenoses;
(3) the upper supply reservoir, the lower collection reservoir, and two identical intermediate circular cylindrical tanks, of height 0·5 m and cross-sectional radius, R, 0·2 m. The intermediate tanks have a thin elastic lateral surface (made from rubber and stiffened with a few vertical ribs), a rigid bottom, and are filled with water to a level $H < 0{\cdot}5$ m. They simulate the human thorax.

The following considerations and assumptions were used in constructing the test section.

Larger blood vessel: Larger human blood vessels can be considered as elastic thin-walled pipes having an inner diameter of approximately 0·1–2cm and a wall thickness–diameter ratio of approximately 0·04–0·13 [3–6, 14, 16, 22]. The silicone elastic pipe was chosen as a model of a larger blood vessel because it allows close matching of geometrical and

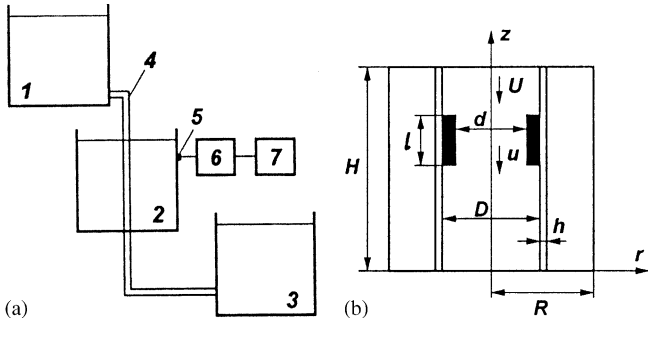

Figure 1. (a) Schematic of experimental system: 1—supply tank; 2—two identical intermediate reservoirs isolated from vibrations; 3—collection tank; 4—two identical silicone pipes (one pipe per reservoir); 5—accelerometer; 6—charge amplifier; 7—frequency analyzer. (b) Schematic of test section.

TABLE 1

Vessel parameters found in periodicals and used in this study

Parameter	D, mm	h, mm	h/D	E_v, N/m^2	ρ_v, kg/m^3	v_v
Silicone pipe	16	2	0·125	$3{\cdot}9 \times 10^5$	$1{\cdot}13 \times 10^3$	0·47
Larger arteries	1–20	0·04–2·6	0·04–0·13	$(1{\cdot}29–10) \times 10^5$	$(0{\cdot}69–1{\cdot}35) \times 10^3$	0·23–0·57

physical parameters (see Table 1), and also because silicone and latex pipes are widely used as a mechanical analogue of blood vessels in both medical practice and *in vitro* studies [14, 16].

Stenosis: The representation of a stenosis as a rigid-walled constriction is justified by the fact that the wall of an arterial stenosis has high stiffness compared with that of the vessel proximal and distal to the stenosis [3–7, 11–14]. As for the axisymmetric abrupt cylindrical geometry of a plug, this is the simplest shape of constriction that allows us to study the role of the most important geometrical characteristics: length and minimum cross-sectional area. In addition, with such an idealization of the shape, one can obtain flow energy distributions behind a stenosis which, in general, look similar to those observable behind real stenotic geometries.

Blood: In this study blood is replaced by water at a temperatute of 20°C. This is a typical replacement in *in vitro* experiments [3–7, 11, 12], because the mass density and the sound speed of normal blood are approximately 1050 kg/m^3 and 1500 m/s, respectively [3, 4], which are very close to those of water. Also blood is usually considered to be an incompressible, homogeneous and (at high shear rates above 50 s^{-1}, commonly found in the larger arteries) Newtonian fluid [3,4]. The difference in viscosity between water and blood is compensated for by the choice of flow velocities at which the blood and water flows are similar in the relevant Reynolds number.

Flow: The frequency range of interest in vascular stenosis murmurs is determined by the parameters of flow, vessel and stenosis, and usually lies between 20 Hz and 1 kHz [5–7, 11–13]. This is high compared with the cardiac cycle frequencies ($\sim$1 Hz). Consequently, the average flow rate changes associated with the cardiac cycle represent a slow variation compared with the relevant disturbed flow fluctuations and associated acoustic field oscillations. As a first order of approximation, we therefore make the usual quasi-steady assumption that during the observation of the disturbed flow and acoustic field fluctuations the flow rate remains essentially unchanged, and consequently the fluctuations depend mainly on the instantaneous flow rate. This investigation therefore focuses on the quasi-steady flow problem with flow rate (or, at constant diameter of the pipe, mean axial flow velocity) as one of the physical parameters.

Thorax: Since the thorax shape is close to cylindrical, and the characteristic dimensions of the thorax and the details of its geometry are small in terms of the acoustic wavelengths of interest in vascular stenosis murmurs, the thorax can be represented by a finite circular cylinder. The height, H, and the cross-sectional radius, R, of such a cylinder can vary in the ranges 0·3–0·6 m and 0·15–0·25 m respectively [23, 24]. Its lateral surface can be considered to be either a thin elastic shell or membrane [21], and its bottom a rigid plane. The latter condition is due to that the average wave resistance of the thorax bottom is much higher than that of body tissue [20]. Another assumption relates to the thorax tissue itself. The available data [20, 21, 23, 24] indicate that the tissue can be considered in the first approximtion as homogeneous acoustic medium with averaged properties. In this experiment water is used as such a medium. Although the acoustic properties of the thorax

tissue and water are different, this difference (actually the difference between the properties of the simulated acoustic channel of noise transmission from vessel to body surface) can be compensated for by the choice of a suitable algorithm in processing the recorded acoustic signal.

The experimental system was operated in the following way. The upper and lower tanks were joined by two pipes passing coaxially through the intermediate reservoirs (one pipe per reservoir). One pipe was smooth and another contained a stenosis. Due to the difference between the levels of water in upper and lower (calibrated in litres) tanks, a flow of mean axial velocity U was created in the vessels (in the partially occluded vessel, U was the velocity of mean flow out of the stenosis region). The velocity U was determined as the ratio of the water volume, Q, accumulated in the collection tank during the period T of data acquisition to the cross-sectional area of the pipe, $A_0 = \pi D^2/4$, and the time T, namely (a list of symbols is given in Appendix A)

$$U = Q/A_0 T. \tag{1}$$

The local mean flow velocity in a stenosis, u, was found from the mass conservation condition in the constricted and intact segments of the pipe, namely

$$uA = UA_0 \tag{2}$$

($A = \pi d^2/4$ is the lumen area of a constriction) to be

$$u = U(A_0/A) = U(D/d)^2. \tag{3}$$

In order to have similarity in the flow Reynolds number, $\mathrm{Re}_D = UD/\nu$, between the experimental flow and real blood flow in a larger vessel, only velocities $U < 0{\cdot}44$ m/s were considered in the experiment. For this velocity range, Re_D was below 7000. These values for Re_D are typical of those found in the larger arteries of the human body such as the ascending aorta and the carotid and femoral arteries [3–7, 13].

A given flow generated noise in each intermediate tank. The noise was measured by an accelerometer (that was developed in reference [21]) resting at the tank lateral surface, and processed by a frequency analyzer. In order to reduce background noise levels, the experiment was conducted in an anechoic chamber. In addition, the intermediate reservoirs were isolated from vibrations. This allowed us to minimize possible contamination of the measured acoustic fields due to sources other than the hydrodynamic pressures under consideration.

3. RESULTS

In this section, the *basic* acoustic effects of a stenosis found in the experiment are presented. The variation of the acoustic power spectrum with the geometrical parameters of the stenosis, mean flow velocity (or the flow Reynolds number) and the vertical distance from the stenosis is also shown. For the moment, we restrict ourselves to a general description of the phenomena observed. Their physics is related to the flow structure and the flow energy distribution in the partially occluded and normal pipes, as well as to the mechanism of transformation of flow energy into acoustic energy, and it is discussed in the next section.

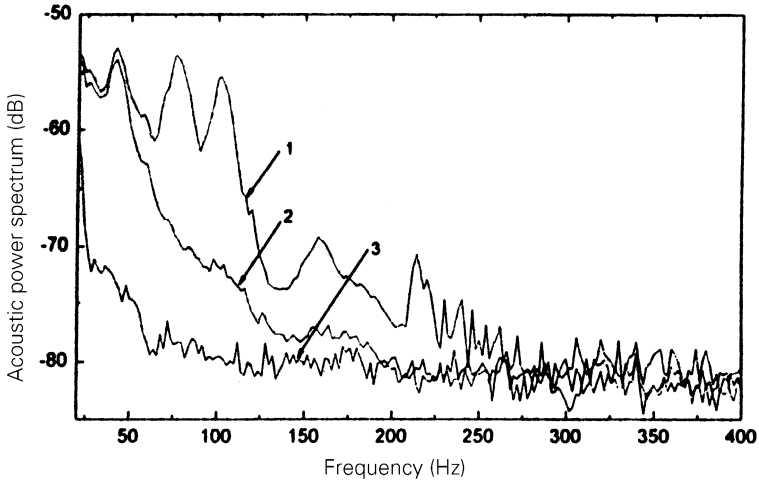

Figure 2. Spectra of the acoustic power produced by flow at a mean velocity $U = 0{\cdot}33$ m/s ($\mathrm{Re}_D = 5280$) and measured at $r = R$, $z = 15$ cm: 1—stenosed pipe ($d = 12$ mm, $l = 20$ mm, $S = 44\%$); 2—normal pipe; 3-background noise.

The axisymmetric geometry of the pipe, stenosis and the intermediate tank, as well as the coaxial position of the pipe in the tank allow one to conclude that the test section exhibits axial symmetry. Also, from the results of studies [2,5,6,8], the flow and wall pressure in both pipes can be considered axisymmetric as a first approximation. Consequently, the acoustic field in each intermediate tank should also be axisymmetric.

This property has been verified by comparison of the acoustic power spectra recorded at different points around the cross-sectional circumference of each tank. The comparison showed that the spectrum was indeed independent of the azimuthal co-ordinate in the frequency range of interest, i.e.,

$$E_{nor}(R, \phi_1, z, f) = E_{nor}(R, \phi_2, z, f),$$

$$E_{ob}(R, \phi_1, z, f) = E_{ob}(R, \phi_2, z, f),\ 20\ \mathrm{Hz} < f < 1\ \mathrm{kHz}. \tag{4}$$

The symmetry of the other statistical characteristics of noise was not checked as they were out of interest in this study.

Some characteristic results obtained under conditions of axial symmetry (4) are presented below. In particular, the power spectra of noise generated by flow of the same mean velocity in the intact and obstructed pipes, and the background noise spectrum are shown in Figure 2. These spectra were measured at the point $r = R$, $z = 15$ cm opposite a stenosis. One can see that, for frequencies below 400 Hz, the level of the stenosis-generated noise is generally higher than that from the uniform pipe, which, in turn, exceeds the background noise level for $f < 190$ Hz. In the frequency range above 400 Hz, the spectra do not practically differ from each other, and no information of interest can be extracted here.

Further analysis of Figure 2 shows that the difference between curves 1 and 2 is strongly dependent on frequency. A few frequency bands can be observed (i.e., $65\ \mathrm{Hz} < f < 85$ Hz, $90\ \mathrm{Hz} < f < 110$ Hz, $144\ \mathrm{Hz} < f < 168$ Hz) where the power of the stenosis-generated noise reaches maxima, while the noise spectrum of the intact vessel is relatively smooth and much lower in level. There are also frequency domains in which both spectra are similar in shape

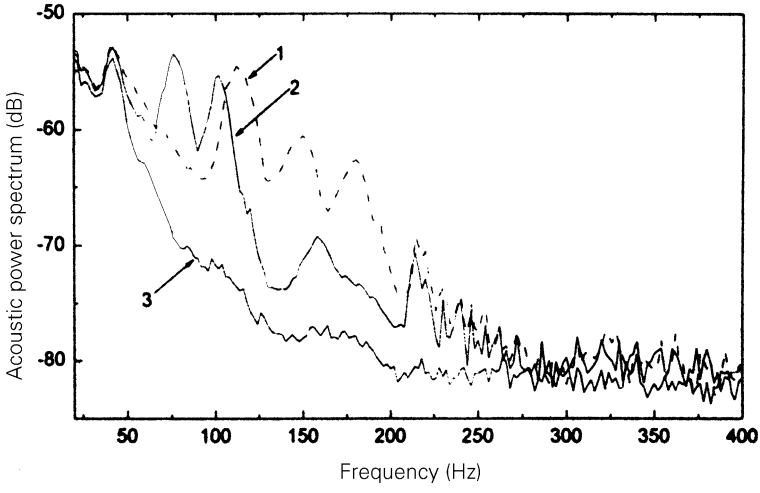

Figure 3. Spectra of the acoustic power produced by flow at a mean velocity $U = 0{\cdot}33$m/s ($\mathrm{Re}_D = 5280$) and measured at $r = R$, $z = 15$ cm: 1—stenosed pipe ($d = 10$ mm, $l = 20$ mm, $S = 61\%$); 2—stenosed pipe ($d = 12$ mm, $l = 20$ mm, $S = 44\%$); 3—normal pipe.

and, the place (i.e., in the domain 35 Hz $< f <$ 50 Hz), where both have maxima of similar amplitude.

Similar changes in the acoustic power spectrum due to a stenosis (i.e., an increase in spectrum level and the appearance of additional distinct peaks) were also observed in all the other recordings made in this study. Consequently, these observations allow us to conclude that a stenosis has *two basic* acoustic effects. These are a general increase in the noise level generated and the production of new frequency components in the power spectrum. The frequencies of the components will be shown in section 4 to be close to the frequencies determined by the parameters of vessel, stenosis and mean flow.

An increase in noise level with a uniform decrease (along the axis) of the pipe diameter has been predicted theoretically in works [23, 24]. The first basic acoustic effect of a constriction can therefore be considered as experimental confirmation and further development of this prediction for the case of a local decrease in the vessel diameter. To the author's knowledge, the second effect has not yet been found, and this is the *main* finding of this study.

Figure 3 presents noise spectra from two stenoses of the same lengths and different inner diameters, and from the intact pipe. All the spectra were produced by flow of the same mean velocity and measured at the point $r = R$, $z = 15$ cm. Apart from the previously noted basic acoustic effects, this figure demonstrates the influence of the constriction severity, S, quantified as

$$S = (1 - A/A_0) \times 100\% = (1 - d^2/D^2) \times 100\%, \tag{5}$$

on both the level of and the positions of the maxima in the acoustic power spectrum. One can see that, firstly, the higher the severity of a stenosis (i.e., the smaller the diameter, d) the higher the noise level generated. Secondly, the locations of some maxima in the stenosis-generated noise spectrum (which are not observed in the spectrum of the unobstructed pipe) depend on S (compare the locations of the maxima in curve 2 in the ranges 65 Hz $< f <$ 85 Hz, 90 Hz $< f <$ 110 Hz, 144 Hz $< f <$ 168 Hz with the locations of the corresponding maxima in curve 1 in the ranges 100 Hz $< f <$ 120 Hz,

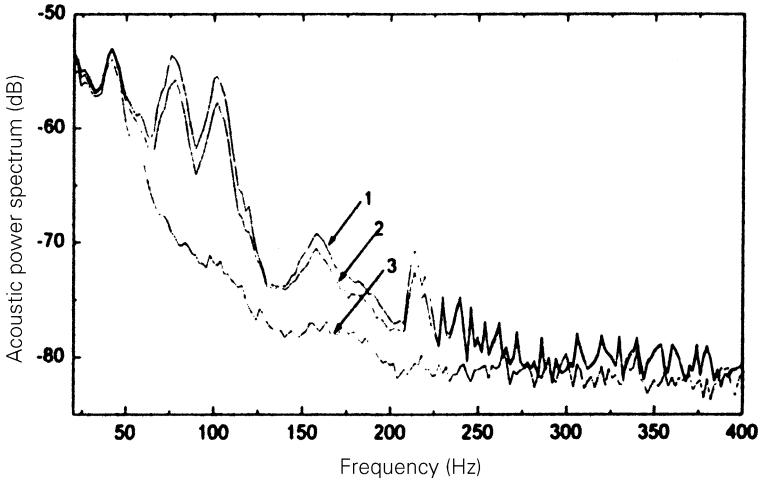

Figure 4. Spectra of the acoustic power produced by flow at a mean velocity $U = 0{\cdot}33$m/s ($\mathrm{Re}_D = 5280$) and measured at $r = R$, $z = 15$ cm: 1—stenosed pipe ($d = 12$ mm, $l = 20$ mm, $S = 44\%$); 2—stenosed pipe ($d = 12$ mm, $l = 40$ mm, $S = 44\%$); 3—normal pipe.

165 Hz $< f <$ 185 Hz, 132 Hz $< f <$ 156 Hz). The locations of the other maxima in curves 1 and 2 (which are not observed in curve 3) are not influenced by S (i.e., the maxima in the domain 210 Hz $< f <$ 400 Hz).

One more frequency band in Figure 3 (i.e., 35 Hz $< f <$ 50 Hz) is notable in that the spectra of noise from the smooth and two stenosed pipes have distinct peaks of close amplitude here. A similar phenomenon has also been detected in Figure 2 and the other recordings made. This indicates that there is an energy-containing frequency component in the acoustic power spectrum which is determined by the basic flow and is practically unaffected by a vessel constriction. The corresponding maximum in the acoustic power spectrum of an originally smooth vessel does not shift and its amplitude increases slightly as a stenosis appears and develops in the vessel.

The role of the constriction length, l, can be seen from Figure 4 where the acoustic power spectra from two stenoses of the same severity and different lengths, and from the intact pipe are presented (as before, all the spectra were generated by flow of the same mean velocity). Comparison of the curves shows that the acoustic power produced by a stenosis decreases/increases as the length l increases/decreases. In other words, the longer the stenosis, the lower the level of acoustic power generated, and vice versa, a shorter stenosis produces noise of higher intensity. The influence of l on the new frequency components is not as evident as that of S.

The dependence of the acoustic power spectrum on mean flow velocity, U (or the flow Reynolds number, Re_D), is seen in Figure 5 to be qualitatively similar to that on constriction severity. Specifically, there is an increase in the noise level and some new frequency components arise due to the increase in U (compare the locations of the maxima in curve 1 in Figure 5(a) in the domains 30 Hz $< f <$ 40 Hz, 45 Hz $< f <$ 60 Hz, 70 Hz $< f <$ 80 Hz with the locations of the corresponding maxima in curve 1 in Figure 5b in the domains 65 Hz $< f <$ 85 Hz, 90 Hz $< f <$ 110 Hz, 144 Hz $< f <$ 168 Hz). The other new frequency components (lying between 210 and 400 Hz) are insensitive to U (namely the locations of the peaks in curve 1 in Figures 5(a) and 5(b) in this frequency range).

The maxima of close amplitude in curves 1 and 2 shift to the right as the velocity U becomes higher (compare the locations of the maxima in Figure 5(a) in the band

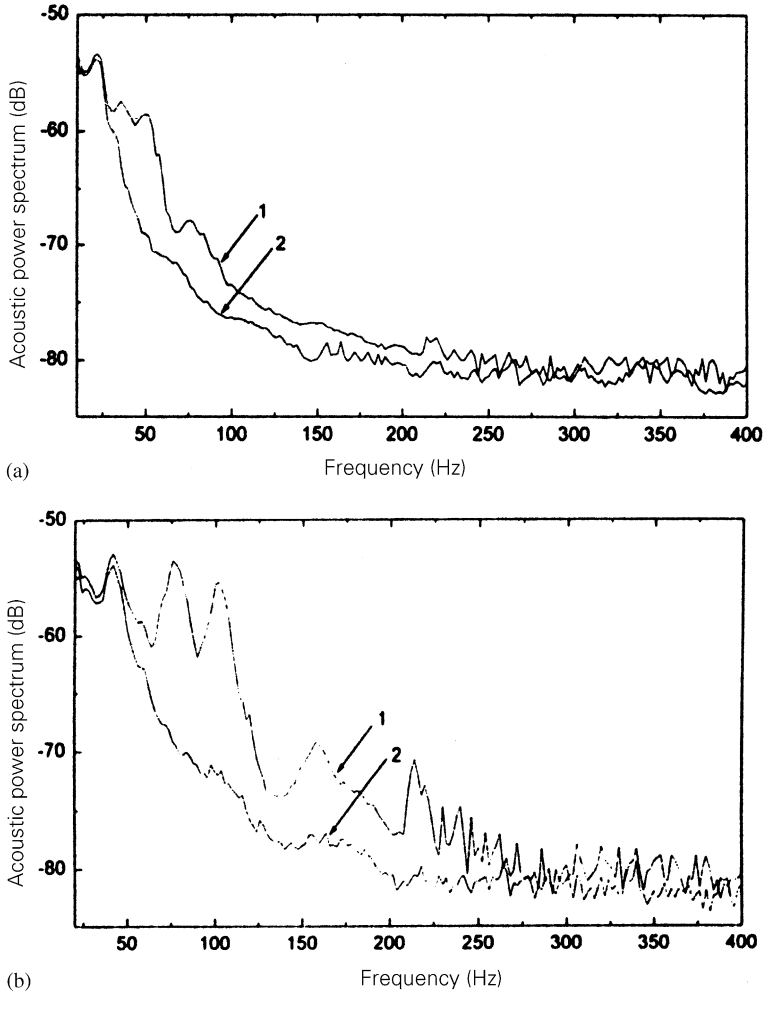

Figure 5. Spectra of the acoustic power (measured at $r = R$, $z = 15$ cm) from stenosed (curve 1: $d = 12$ mm, $l = 20$ mm; $S = 44\%$) and normal (curve 2) pipes: (a) $U = 0{\cdot}16$ m/s ($\mathrm{Re}_D = 2560$); (b) $U = 0{\cdot}33$ m/s ($\mathrm{Re}_D = 5280$).

15 Hz $< f <$ 25 Hz with the locations of the maxima in Figure 5(b) in the range 35 Hz $< f <$ 50 Hz). Another feature of Figure 5 is that not only does the level of noise from both pipes increase, but also the difference between the levels of noise from the stenosed and normal pipes increases with velocity U. The difference is seen to be rather sensitive to small changes in U.

The variance of the spectrum $E_{ob}(R, z, f)$ with the vertical distance from a stenosis is demonstrated in Figure 6. Here all the data were produced by the same stenosis at the same mean flow velocity and measured at different points along the generator of the lateral surface of the test section. It can be seen that the level of noise decreases as the distance increases, while the locations of the pronounced maxima in and the shapes of the curves are practically the same.

Figures 3 and 5 showed the variation of the acoustic power spectrum with the stenosis severity and the flow Reynolds number, respectively. It was seen that, apart from the other

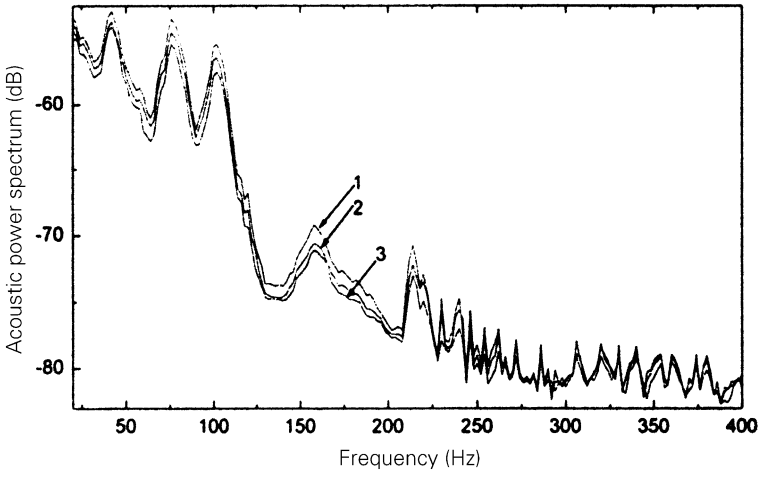

Figure 6. Variation of the spectrum $E_{ob}(R, z, f)$ with vertical distance from a stenosis ($d = 12$ mm, $l = 20$ mm, $S = 44\%$, $U = 0{\cdot}33$ m/s, $\mathrm{Re}_D = 5280$): 1—$z = 15$ cm, 2—$z = 5$ cm, 3—$z = 35$ cm.

effects, increases in the constriction severity and/or the Reynolds number caused an increase in the intensity of the acoustic field. Those observations were of qualitative character. In order to have quantitative estimates of the dependence of the power spectrum E_{ob} on these parameters, the relationship between E_{ob}, recorded at the point ($r = R$, $z = 15$ cm) , the Reynolds number Re_D and the area ratio, A_0/A, was assumed to be of the form

$$E_{ob} = K(A_0/A)^{\alpha}(\mathrm{Re}_D)^{\beta}, \tag{6}$$

and the parameters K, α and β were calculated from a linear regression analysis. It was found that, if the spectrum E_{ob} was scaled with the parameter $(A_0/A)^4$ (i.e., $\alpha = 4$), the data for stenoses of differing severities could be reduced to approximately a single curve $K\mathrm{Re}_D^{4{\cdot}4}$ (i.e., $\beta = 4{\cdot}4$) as shown in Figure 7. The parameter K and the relative deflection coefficient ζ, calculated from the expression

$$\zeta = \sum_{i=1}^{N} \frac{\zeta_i}{N}, \quad \zeta_i = \left| 1 - \frac{K(A_0/A)^4(\mathrm{Re}_D)^{4{\cdot}4}}{E_{ob}} \right|_{\mathrm{Re}_D = \mathrm{Re}_{Di}}$$

(N is the number of measurements) were equal to $1{\cdot}93 \times 10^{-24}$ and 0·102 (Figure 7(a)), and $2{\cdot}44 \times 10^{-25}$ and 0·114 (Figure 7(b)), respectively. Thus, the relationship between the stenosis generated noise spectrum measured at the point $r = R$, $z = 15$ cm, the degree of constriction and the flow Reynolds number can be expressed as

$$E_{ob} = K(A_0/A)^4(\mathrm{Re}_D)^{4{\cdot}4} = K(D/d)^8(\mathrm{Re}_D)^{4{\cdot}4}, \tag{7}$$

where the coefficient K is a function of the pipe-wall properties, boundary conditions, frequency, calibration factor for the measuring system, etc. Since the shape of the spectrum E_{ob} was found in the experiment to depend weakly on the vertical distance from the stenosis (see Figure 6), one can conclude that the general dependence of $E_{ob}(R, z, f)$ on A_0/A and Re_D will be of the form (7).

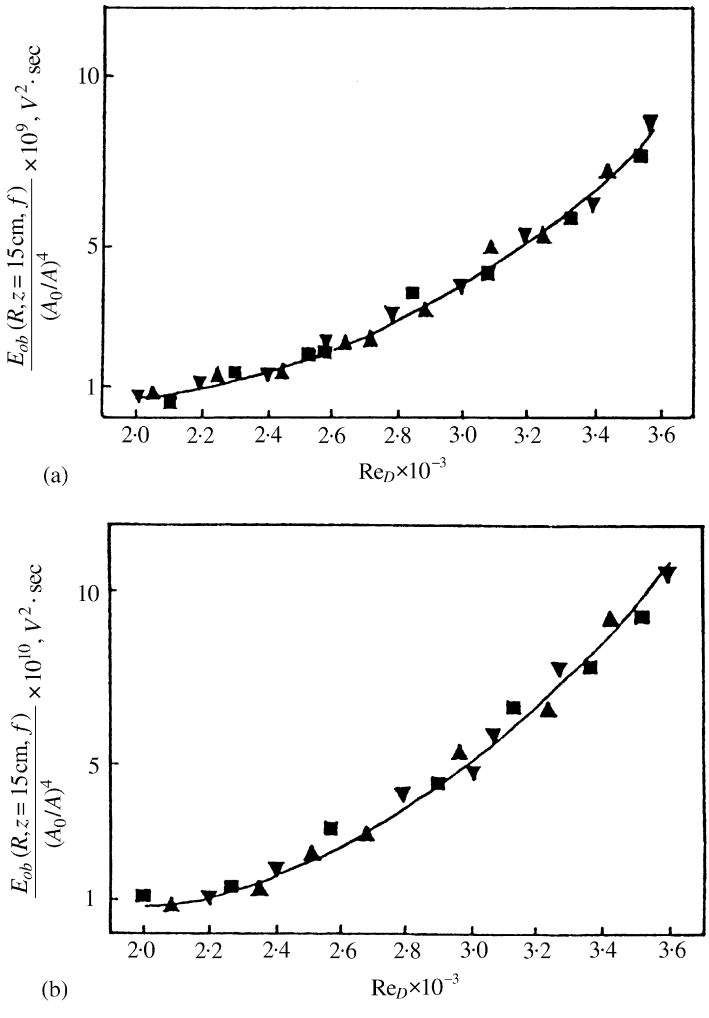

Figure 7. Spectrum $E_{ob}(R, z = 15\text{ cm}, f)$ normalized by $(A_0/A)^4$ versus Reynolds number Re_D: ▲—$S = 34\%$, ■—$S = 44\%$, ▼—$S = 53\%$; solid line—$K(\text{Re}_D)^{4\cdot4}$, (a) $f = 75$ Hz, $K = 1{\cdot}93 \times 10^{-24}$, $\zeta = 0{\cdot}102$; and (b) $f = 125$ Hz, $K = 2{\cdot}44 \times 10^{-25}$, $\zeta = 0{\cdot}114$.

4. ANALYSIS OF THE RESULTS

The data presented in section 3 can be explained on the basis of the flow structure and energy distribution in the stenosed and intact pipes, and the mechanism of transformation of flow energy into acoustic energy. In making this explanation, only basic flow regimes in the pipes are considered, and only large-scale vortex structures are taken into account. These structures contain the main part of the flow energy, and their contribution was shown in references [17–19] to dominate the acoustic fields produced by turbulence-excited elastic elements. Small-scale vortices are omitted, because (i) only a little of the flow energy is distributed among them, (ii) small eddies are characterized by higher frequencies than large eddies, and therefore contribute mainly to the high-frequency range of the acoustic power spectrum, which is usually dominated by background noise (as in Figure 2 in the frequency range above 400 Hz).

Although the further analysis (which is based on such simplified argumentations of the flow, etc.) is not fully rigorous, it nevertheless allows us generally to understand the basic acoustic effects of a stenosis found in section 3 and establish correlation between these effects and the parameters of vessel, stenosis and flow. In order to obtain more sophisticated correlations and reveal the higher order acoustic effects of a constriction (and quantitatively describe them), it would be necessary to carry out a more sophisticated experiment, probably including flow visualization, etc. In analyzing the results of such an experiment, it would be necessary to consider small-scale vortex structures, such as those due to Kelvin–Helmholtz instability of the shear layer bending the main separation region behind a stenosis, etc.

4.1. FLOW STRUCTURE AND FLOW ENERGY DISTRIBUTION IN THE STENOSED AND INTACT PIPES

Upstream of the stenosis (zone 1 in Figure 8), the steady flow is like that in the intact pipe. Here it has mean axial velocity U, and is either laminar or turbulent depending on the flow Reynolds number, Re_D. When Re_D exceeds the critical Reynolds number for the development of turbulence in pipe, Re_{cr}, the flow is turbulent and produces noise. The main part of the flow energy in zone 1 is distributed among large-scale eddies of sizes of order $D/2$ which are convected at speeds of order U and are characterized by frequencies of order

$$f_{ch}^{(1)} = 2U/D. \tag{8}$$

Large turbulent vortex structures were shown in references [17–19] to determine the energy-containing low-frequency domain of the wall pressure power spectrum. This spectrum was found in references [10, 16] to have a maximum in this domain (see Figure 9), and the frequency of the maximum can be attributed to the characteristic frequency of the large turbulent eddies. Consequently, one can conclude that the power spectrum of the wall pressure in zone 1 should exhibit a low-frequency maximum in the range determined by the characteristic frequency $f_{ch}^{(1)}$, namely

$$f \pm \Delta f = O(f_{ch}^{(1)}), \quad \Delta f/f < 1. \tag{9}$$

When $\mathrm{Re}_D < \mathrm{Re}_{cr}$, the fluid motion upstream of the stenosis is laminar. Steady laminar flow should not produce noise. If noise is generated by the experimental flow in zone 1 at

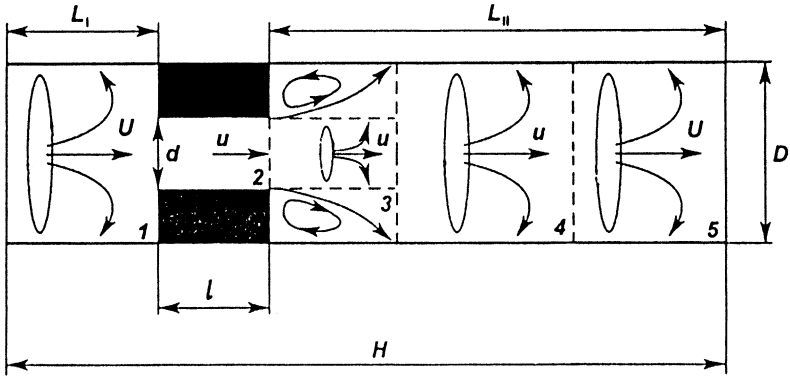

Figure 8. Schematic of the flow structure in the stenosed pipe.

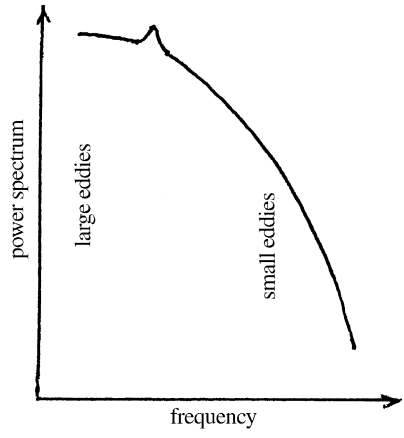

Figure 9. Sketch of the turbulent wall pressure power spectrum based on the data reported in references [10, 16–19].

$\mathrm{Re}_D < \mathrm{Re}_{cr}$, no flow structure can be definitely identified as containing the bulk of the flow energy. Therefore, the wall pressure power spectrum should not exhibit distinguishable maximum at any frequencies.

As the fluid flows into the sharp-edged axisymmetric constriction (zone 2 in Figure 8), it is disturbed and characterized by mean axial velocity $u = U(D/d)^2$. Immediately after the abrupt constriction (zone 3), the disturbed flow usually separates and, as was shown in reference [1–4, 8, 10], has an axisymmetric jet-like form, with jet core diameter d and centreline velocity u. A disturbed flow in zone 3 becomes turbulent when the jet Reynolds number exceeds the required critical value. In both flow regimes, noise is generated.

The main part of the flow energy in the separation region is distributed among two groups of large-scale eddies. The eddies constituting one group occupy the jet region. They move at speeds of order u, have sizes of order $d/2$ and frequencies of order

$$f_{ch}^{(2)} = 2u/d. \tag{10}$$

Another group of large-scale vortices is located in the recirculating flow region near the pipe wall. They have dimensions of order $(D - d)/2$ and can be characterized by frequencies of order

$$f_{ch}^{(3)} = 2u_c/(D - d), \tag{11}$$

where $u_c \sim 0{\cdot}45$–$0{\cdot}6u$ is a convection velocity on the outer side of the shear layer [10, 16, 25, 26]. Taking into account the arguments used for zone 1 one can conclude that the power spectrum of wall pressure in zone 3 should exhibit two peaks in the low-frequency ranges determinable by frequencies (10) and (11), namely

$$f \pm \Delta f = O(f_{ch}^{(2)}),\ f \pm \Delta f = O(f_{ch}^{(3)}). \tag{12}$$

After reattachment (zone 4 in Figure 8), the centreline velocity was noted in the introduction to remain close to the velocity u within the obstruction. The fluid state in zone 4 is either disturbed or turbulent, and noise is produced in these flow regimes. The bulk of

the flow energy is distributed among large-scale eddies of dimensions of order $D/2$, which are convected at speeds of order u and have frequencies of order

$$f_{ch}^{(4)} = 2u/D \,. \tag{13}$$

Following the arguments used for zones 1 and 3 one can come to the conclusion that the wall pressure power spectrum in zone 4 should exhibit a maximum in the energy-containing low-frequency domain, the frequency of the maximum falling in the range determined by frequency (13), namely

$$f \pm \Delta f = O(f_{ch}^{(4)}). \tag{14}$$

When separation does not occur behind a stenosis, zones 3 and 4 constitute a finite region of either disturbed or turbulent flow in which the wall pressure power spectrum should be characterized by a maximum in the frequency range (14).

Since the constricted pipe is sufficiently long and of constant diameter downstream from the plug, the flow in zone 5 gradually redevelops into the basic flow upstream of the plug [3, 4], with the corresponding energy distributions.

Of the five domains identified, domains 3 and 4 have the most intensive flow fluctuations and hence the most intensive noise sources (wall pressure fluctuations). In terms of the energy distribution in frequency, this means that the power spectrum of the wall pressure in zones 3 and 4 is generally either higher or much higher in level (depending on the stenosis severity) than that in regions 1 and 5 and in the intact pipe.

Since the flow in regions 1 and 5 is similar to that in the intact pipe, the wall pressure field and its spectral characteristics in the intact pipe are similar to those in regions 1 and 5 of the stenosed pipe.

4.2. ACOUSTIC EFFECTS OF A STENOSIS

In this section, we shall identify the factors governing the acoustic field in the test volume, and show the changes in these factors that are caused by a stenosis. These changes will then be related to the alterations in the acoustic power spectrum that were found in section 3. We will concentrate on the basic acoustic effects of a stenosis, namely the increase in noise level and appearance of additional maxima in the acoustic power spectrum.

4.2.1. *Basic acoustic effects*

In references [23, 24] it was shown that the acoustic field in a closed volume between a finite pipe and external finite coaxial cylinder, due to flow-wall interaction in the pipe, is determined by (i) the flow energy (or by the wall pressure spectrum); (ii) the efficiency of excitation of the pipe vibration by wall pressure; (iii) the pipe resonant properties; (iv) the degree of spatial correlation of the pipe normal modes with the acoustic modes of the volume; (v) the acoustic properties of the medium in the volume.

It is logical to conclude that these factors also specify the acoustic field in our case.

The appearance of a stenosis in the pipe does not influence the acoustic properties of the medium in the test volume. However, it does cause strong changes in the flow energy. Firstly, the energy (and the wall pressure amplitude or the level of wall pressure spectra) increases in zones 3 and 4. This automatically results in a general growth of the amplitude of the pipe vibration (via the increase in the eficiency (ii)) and hence, in a general growth of the

radiated sound power. Such a variation in the acoustic field due to a constriction was observed in section 3, where it was identified as the first basic acoustic effect of a stenosis.

Secondly, with the plug inserted, the flow energy in zones 3 and 4 is redistributed among the vortices discussed in section 4.1. This leads to the appearance of the additional maxima in the wall pressure power spectrum in frequency bands (12) and (14) (note that, at $\mathrm{Re}_D \geqslant \mathrm{Re}_{cr}$, this spectrum already has a low-frequency peak in range (9)). These maxima are then reflected in the acoustic power spectrum E_{ob}. Since the spectrum of the intact pipe, E_{nor}, does not exhibit maxima in domains (12) and (14), these peaks can be attributed to one set of the new frequency components found in section 3. Their appearance was identified as the second basic acoustic effect of a stenosis.

Apart from the variations in (i), a stenosis also results in changes in the vibration field of the pipe. Specifically, since a stenosis is essentially a rigid baffle, the total field consists of the vibration fields of the pipe segments upstream and downstream of the constriction (segments I and II in Figure 8). Each segment has its own resonance frequencies (which differ from the resonance frequencies of the intact pipe), and the acoustic power spectrum of the partially occluded pipe, E_{ob}, should have maxima at these frequencies. These maxima cannot be found in the spectrum of the normal pipe, E_{nor}, and consequently, they can be identified as another set of new frequency components produced by a stenosis. Here it is most likely that only the natural frequencies of the post-stenotic segment of the vessel contribute to this set. This is because under the laminar basic flow condition, $\mathrm{Re}_D < \mathrm{Re}_{cr}$, the flow energy in segment I is not transformed into sound and hence, the spectrum E_{ob} should not exhibit maxima at the natural frequencies of segment I; under the turbulent basic flow condition, $\mathrm{Re}_D \geqslant \mathrm{Re}_{cr}$, the spectrum E_{ob} should have maxima at the natural frequencies of segment I; however, these maxima should be either lower or much lower (depending on the stenosis severity) than the maxima at the natural frequencies of segment II (because the energy of flow in segment II is either higher or much higher than that in segment I and hence, the amplitude of vibration of segment II should be either higher or much higher compared with that of segment I).

It should be noted that the indicated changes in the vibration field of the vessel automatically cause changes in (ii) and (iv) (because the normal modes of the stenosed pipe differ from those of the intact pipe). However, neither of these changes are dominant for either the increase in noise level or the production of new frequency components found in the experiment.

In order to verify our arguments regarding the new frequency components, we firstly compared the characteristic frequencies $f_{ch}^{(2)}, \ldots, f_{ch}^{(4)}$ and the resonance frequencies of pipe segment II with the frequencies of the additional maxima due to a stenosis that were found in the acoustic power spectrum in Figure 2. The following values of the test section parameters were used:

$$U = 0{\cdot}33 \text{ m/s}, \nu = 10^{-6} \text{ m}^2/\text{s}, \mathrm{Re}_D = 5280, d = 12 \text{ mm}, l = 20 \text{ mm}, S = 44\%, H = 0{\cdot}4 \text{ m}.$$

The other magnitudes are given in section 2. The natural frequencies of pipe segment II were computed from the expression for the resonance frequencies of axisymmetric flexural vibration of a simply supported thin-walled circular pipe which is surrounded by a finite coaxial circular cylinder (the space between the cylinders is filled with an acoustic medium; the lower and upper sides of such a closed cylindrical system are rigid and pressure-released planes, respectively, and the lateral surface is preassure-released), namely [27]

$$f_{n*}^{(j)} = f_n^{(j)} / \sqrt{1 + m_n^{(j)} / \rho_v h}\,, \tag{15}$$

TABLE 2

Frequency of the additional maxima in the range below 210 Hz

Found in Figure 2 (Hz)	$f \pm \Delta f = 65$–85	$f \pm \Delta f = 90$–110	$f \pm \Delta f = 144$–168
Predicted (Hz)	$f_{ch}^{(4)} = 73{\cdot}33$	$f_{ch}^{(2)} = 97{\cdot}78$	$f_{ch}^{(3)} = 132$–176

TABLE 3

Frequency of the additional maxima in the range above 210 Hz

n	1, …, 8	10, 11	13, 14	15	16
Predicted, $f_n^{(\mathrm{II})}$ (Hz)	214·08, …, 216·33	219·54, 222·02	229·32, 234·35	240·43	247·66
Found in Figure 2 (Hz)	214	220	230	240	246
n	17	18	19	20	21
Predicted, $f_n^{(\mathrm{II})}$ (Hz)	256·1	265·83	276·88	289·28	303·05
Found in Figure 2 (Hz)	254	262	272	286	306

in which

$$f_n^{(j)} = \frac{c_v}{2\pi a}\sqrt{1 + (k_n^{(j)}a)^4\frac{h^2}{12a^2}}$$

are the *in vacuo* resonance frequencies of a simply supported pipe (the jth pipe segment),

$$m_n^{(j)} = \frac{1}{2\pi f}\mathrm{Im}(Z_n^{(j)})$$

the added mass of the nth normal mode of the jth pipe segment (defined as the imaginary part of the radiation impedance of the mode

$$Z_n^{(j)} = \mathrm{i}\rho_0 2\pi f\left(\frac{2}{L_j}\right)^2\sum_{m=1}^{\infty}\frac{1}{\alpha_m}\frac{F(\alpha_m, a, R)}{G(\alpha_m, a, R)}\frac{k_n^{(j)2}}{(k_n^{(j)2} - \gamma_m^2)^2},$$

divided by the circular frequency $2\pi f$),

$$F(\alpha_m, a, R) = \mathrm{J}_0(\alpha_m a)\,\mathrm{Y}_0(\alpha_m R) - \mathrm{Y}_0(\alpha_m a)\,\mathrm{J}_0(\alpha_m R),$$

$$G(\alpha_m, a, R) = \mathrm{Y}_1(\alpha_m a)\,\mathrm{J}_0(\alpha_m R) - \mathrm{J}_1(\alpha_m a)\,\mathrm{Y}_0(\alpha_m R),$$

the combinations of cylindrical Bessel functions, i the complex unity ($\mathrm{i}^2 = -1$), ρ_0 the mass density of the acoustic medium between the coaxial cylinders, $c_v = \sqrt{E_v/\rho_v(1 - v_v^2)}$ the longitudinal wave speed in the pipe wall, $a = (D + h)/2$ the radius of the midsurface of the pipe, $\gamma_m = (2m - 1)\pi/2H$ the wavenumber of the mth acoustic mode of the volume between the cylinders, $\alpha_m = \sqrt{k_0^2 - \gamma_m^2}$ the radial wavenumber, $k_0 = 2\pi f/c_0$ the acoustic wavenumber, c_0 the sound speed in the acoustic medium, and $k_n^{(j)} = n\pi/L_j$ and L_j the modal wavenumber and length of the jth pipe segment, respectively (j = I,II).

TABLE 4

Frequency of the additional maxima in the range above 210 Hz

n	1, … , 13	14, 15, 16	20, 21	23	24
Predicted, $f_n^{(I)}$ (Hz)	214·08, … , 216·91	217·89; 219·08; 221·28	229·52; 232·71	240·43	245·01
Found in Figure 2 (Hz)	214	220	230	240	246

TABLE 5

Frequency of the maxima of close amplitude in the spectra E_{ob} *and* E_{nor}

Found in Figure 2 (Hz)	Predicted (Hz)
$f \pm \Delta f = 35$–50	$f_{ch}^{(1)} = 41{\cdot}25$

The results of such a comparison are pesented in Tables 2 and 3. The correlation between the theoretical and experimental values is seen to be rather good. Similar results were also obtained for the other configurations of the test section. The correlation was always good for the natural frequencies $f_n^{(II)}$; for the characteristic frequencies $f_{ch}^{(2)}, \ldots, f_{ch}^{(4)}$, it was sometimes worse, but fairly satisfactory over all.

Secondly, we inserted a small grid (with square-shaped orifices of dimensions less than $d/3 \times d/3$) in the outlet section of the stenosis and attached additional mass to the post-stenotic segment of the pipe. The grid was expected to destroy the large-scale vortex structures in the disturbed flow region behind the stenosis and change both the structure and dimensions of the recirculation flow region. This should have resulted in the disappearance of the maxima in the spectrum E_{ob} at the characteristic frequencies $f_{ch}^{(2)}, \ldots, f_{ch}^{(4)}$. The additional mass increases the average mass density of the segment wall, ρ_v, and hence, should decrease the resonance frequencies $f_n^{(II)}$. As a result, the maxima in the spectrum E_{ob} at $f_n^{(II)}$ were expected to shift to the left. All these effects were observed in the experiment.

The resonance frequencies of pipe segment I, calculated from expression (15), also fall in the range 210 Hz $< f <$ 400 Hz (see Table 4). However, no shift of the maxima in E_{ob} in this frequency band was observed when the mass was attached to segment I.

Thus, these arguments confirm the identification, in the first approximation, of the frequencies $f_{ch}^{(2)}, \ldots, f_{ch}^{(4)}$ and $f_n^{(II)}$ with the *new* frequency components produced by a vascular constriction. In order to obtain more sophisticated corelation between the frequencies of the additional maxima in the spectrum E_{ob} and the parameters of flow, vessel and stenosis, it would be necessary, as was noted at the beginning of section 4, to carry out a more sophisticated experiment.

Finally, it should be said that the agreement between the characteristic frequency $f_{ch}^{(1)}$ and the frequency of the maxima of similar amplitude in the spectra E_{ob} and E_{nor}, measured under the condition $\mathrm{Re}_D \geqslant \mathrm{Re}_{cr}$, was also rather good for the various configurations of the test section (see Table 5). A value of 2000 for the critical Reynolds number for the development of turbulence in the pipe (the maximum of those reported in periodicals [3, 4, 23, 24, 28]) was chosen here. Under the laminar flow condition, $\mathrm{Re}_D < \mathrm{Re}_{cr}$, we were unable to detect a maximum in both spectra in the vicinity of the frequncy $f_{ch}^{(1)}$.

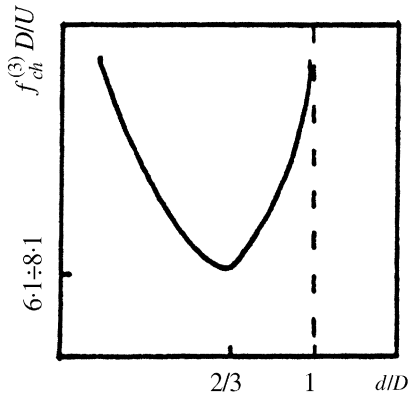

Figure 10. Variation of the frequency $f_{ch}^{(3)}$ with d.

4.2.2. *Effects of the geometrical parameters of a stenosis*

The effects of the geometrical parameters of the stenosis on the acoustic power spectrum (demonstrated in Figures 3 and 4) can be explained on the basis of the physics of the basic acoustic effects. In fact, increase in the constriction severity (5) (or a decrease in d) causes an increase in both velocity (3) and wall pressure amplitude in the disturbed flow region behind the stenosis (domains 3 and 4 of Figure 8). Also the length of this region has been shown [1, 3–6, 22] to grow as S increases. This leads, on the one hand, to an increase in the amplitude of vibration of the pipe segment II and hence, to a general growth in the noise level generated (see Figure 3 and the corresponding comments in section 3). On the other hand, the characteristic frequencies $f_{ch}^{(2)}$ and $f_{ch}^{(4)}$ can be seen from expressions (10) and (13) to become higher as the constriction diameter decreases. Accordingly, the maxima in the spectrum E_{ob} around these frequencies shift to the right, as was found in Figure 3.

The variation of the frequency $f_{ch}^{(3)}$ with d is shown in Figure 10. This plot explains the dependence of the position of the maximum in the function E_{ob} around $f_{ch}^{(3)}$ on the stenosis severity (found in Figure 3 and in the other appropriate recordings of this study).

Since the resonance frequencies of the pipe segment II are independent of the stenosis diameter, the locations of the maxima in the spectrum E_{ob} in the frequency band between 210 and 400 Hz remain unchanged as S varies.

The stenosis length, l, controls the influence of fluid viscosity on the disturbed flow in zone 2. If l grows, this influence increases and hence, the dissipation of flow energy in zone 2 increases. This results in lower noise sources intensity in zones 3 and 4. Also the effective radiating surface of the obstructed pipe decreases as l increases. The lower the noise source intensity in, and the smaller the effective radiating surface of the stenosed pipe, the less acoustic energy is radiated (see Figure 4).

The characteristic frequencies $f_{ch}^{(2)}, \ldots, f_{ch}^{(4)}$ are seen from expressions (10), (11) and (13) to be independent of l. Accordingly, the locations of the peaks in the spectrum E_{ob} around these frequencies are not changed as l increases or decreases. The resonance frequencies $f_n^{(II)}$ depend very weakly on the stenosis length (via the relationship $L_{II} = H - L_I - l$). As a result, the shift of the maxima in the spectrum E_{ob} at the frequencies $f_n^{(II)}$ due to a change in the stenosis length is practically imperceptible, as was found in Figure 4.

4.3. VARIATION OF THE SPECTRUM E_{ob} WITH z, Re_D AND A_0/A

The variation of the spectrum E_{ob} with vertical distance from a stenosis (as shown in Figure 6) can be explained by the non-uniform axial distribution of flow energy (and wall pressure) in the obstructed pipe. In fact, this non-uniformity of the sound sources causes a corresponding non-uniformity of the acoustic field in the axial co-ordinate, z. Since the most powerful sound sources lie in the disturbed flow (regions 3 and 4 in Figure 8), the maximum acoustic level at the lateral surface of the test section can be heard in a finite circular segment opposite that region. The height of the segment is strongly correlated with the length of the region.

The empirical expression (7), relating the acoustic power spectrum E_{ob} to the stenosis severity and the flow Reynolds number, can also be deduced from the following arguments. The pressure fluctuations in the pipe flow, p_t, are directly proportional to the fluid mass density, ρ_f, and the second power of mean flow velocity, U_f, i.e., [19]

$$p_t \sim \rho_f U_f^2.$$

The wall pressure power spectrum, quantified as the second statistical moment of p_t [17–19], is proportional to $\rho_f^2 U_f^4$. Consequently, one can write

$$P_r \sim \rho^2 U^4, \quad r = 1, 5; \; P_q \sim \rho^2 u^4, \quad q = 3, 4$$

for the power spectra of wall pressure in the radiating flow regions in Figure 8. Substituting expression (3), we have

$$P_q \sim \rho^2 U^4 (A_0/A)^4 = \rho^2 U^4 (D/d)^8, \quad q = 3, 4. \tag{16}$$

The acoustic field from the partially occluded pipe is dominated by the contribution from segment II, i.e.,

$$E_{ob} = E_{\mathrm{I}} + E_{\mathrm{II}} \approx E_{\mathrm{II}}. \tag{17}$$

The spectrum E_{II} produced by the pipe segment II can be written in the form

$$E_{\mathrm{II}} = T \times (P_3 + P_4 + P_5) \approx T \times (P_3 + P_4), \tag{18}$$

where T is a function reflecting the properties described in items (ii)–(v) of section 4.2.1.

Substituting equation (18) into equation (17) and taking into account equation (16), we see that the acoustic power spectrum of the stenosed pipe is approximately determined by the fourth power of the mean flow velocity, U, and the same power of the area ratio, A_0/A, namely

$$E_{ob} \approx T \times (P_3 + P_4) \sim T \times \rho^2 U^4 (A_0/A)^4 = T \times \rho^2 U^4 (D/d)^8.$$

Introducing the fluid viscosity, v, in this relationship gives

$$E_{ob} \sim (\mathrm{Re}_D)^4 (A_0/A)^4 \times T\rho^2 v^4/D^4 = (\mathrm{Re}_D)^4 (D/d)^8 \times T\rho^2 v^4/D^4.$$

For a given pipe, fluid and acoustic medium in the test section, $T\rho^2 v^4/D^4$ is constant and therefore

$$E_{ob} \sim (\mathrm{Re}_D)^4 (A_0/A)^4 = (\mathrm{Re}_D)^4 (D/d)^8, \tag{19}$$

which is relationship (7), with the exponent of Re_D increased slightly to give a better fit to the data.

Using similar arguments, one can obtain an estimate for the difference in acoustic power produced by the stenosed and intact pipes, ΔE, namely

$$\Delta E \sim (\mathrm{Re}_D)^4[(A_0/A)^4 - 1] = (\mathrm{Re}_D)^4[(D/d)^8 - 1]. \tag{20}$$

The difference is seen to increase as the flow Reynolds number, Re_D, and/or the area ratio, A_0/A, increase. This effect was shown in Figures 3 and 5.

Writing the ratio of the acoustic power spectra from two stenoses of differing severities, E_1 and E_2, we have

$$E_1/E_2 \sim A_2^4/A_1^4 = d_2^8/d_1^8 .$$

This relationship indicates that an approximately two-fold decrease in the cross-sectional area of the vessel (i.e., $A_2/A_1 \sim 1{\cdot}78$) causes a 10-fold increase in the radiated acoustic power (one order of magnitude).

5. PRACTICAL IMPORTANCE OF THE RESULTS

Among the results of this study, the basic acoustic effects of a stenosis can be of the most practical interest, although the other effects may also be important.

5.1. BASIC ACOUSTIC EFFECTS OF A STENOSIS

These effects can be detected from analysis of the acoustic field recorded periodically from a patient, and their appearance in the acoustic power spectrum of an originally healthy vessel can indicate the local reduction in the lumen area of vessel. Further increases (during the monitoring of the patient) in the acoustic power level and shifts (to the right) of some of the additional distinct peaks in the spectrum due to a stenosis will indicate progressions in the stenosis severity.

The correlations between the frequency of the additional maxima and the parameters of vessel, stenosis and mean flow (expressions (10), (11) and (13)) can be used for finding (as a first approximation) the stenosis diameter. The calculation proceeds as follows. Firstly, it is necessary to relate the frequency of the additional maxima in the acoustic power spectrum to the corresponding characteristic frequencies of vortex formation in the disturbed flow region behind a stenosis (i.e. to $f_{ch}^{(2)}$, $f_{ch}^{(3)}$, $f_{ch}^{(4)}$). Then, if the mean flow velocity in the vessel under investigation is known, the stenosis diameter can be approximately determined either from (10) or (13), namely

$$d \sim (2UD^2/f_{ch}^{(2)})^{1/3}, \qquad d \sim (2UD/f_{ch}^{(4)})^{1/2}. \tag{21}$$

If the velocity U is unknown, the diameter d can be found, for example, from the system of equations (10) and (13), namely

$$d \sim (f_{ch}^{(4)}/f_{ch}^{(2)})\, D. \tag{22}$$

Other pairings of equations (10), (11) and (13) will give us additional approximate estimates for the stenosis diameter. The real value of d should be close to these estimates.

Another estimate for the constriction diameter can be obtained from relationships (7) and (20). The acoustic power produced by an originally healthy vessel, Π_{nor}, can be written as

$$\Pi_{nor} \approx K_*(\mathrm{Re}_D)^{4\cdot4}$$

from which the coefficient K_* is determined as

$$K_* \approx \Pi_{nor}/(\mathrm{Re}_D)^{4\cdot4}.$$

The difference $\Delta\Pi$ between the acoustic powers from an originally healthy (Π_{nor}) and subsequently stenosed (Π_{ob}) vessel can be written in the form

$$\Delta\Pi = \Pi_{ob} - \Pi_{nor} \approx K_*(\mathrm{Re}_D)^{4\cdot4}[(D/d)^8 - 1],$$

or, taking into account the above estimate for the coefficient K_*,

$$\Delta\Pi = \Pi_{ob} - \Pi_{nor} \approx \Pi_{nor}[(D/d)^8 - 1].$$

Consequently, the diameter d is

$$d \sim D(\Pi_{nor}/\Pi_{ob})^{1/8}. \tag{23}$$

5.2. ANOTHER EFFECTS

There can exist cases when the longitudinal dimension of a detectable mild constriction grows with time, and the constriction severity remains unchanged. This can lead to a decrease in the generated noise level (as shown in Figure 4), and hence to reduced differences between the recordings of noise made previously (when the vessel was healthy) and currently (when it contains a stenosis). Consequently, there can exist situations when, on reaching some critical value of stenosis length, $l = l_{cr}$, the difference between the noise level from healthy and diseased vessels becomes so small that a previously detectable stenosis becomes practically undetectable by acoustic diagnosis techniques. The only remaining signs of a stenosis may now be the new frequency components, if distinguishable. If the components cannot be distinguished, a vascular lesion cannot then be detected. These considerations look reasonable, and can stimulate researchers towards establishing the quantitative relationship between l_{cr} and the parameters of flow, vessel and stenosis.

The increase in the difference between the levels of noise from stenosed and normal pipes due to a increase in mean flow velocity (shown in Figure 5) suggests that it may be better to detect stenoses under elevated flow conditions (manual labour) rather than under normal flow conditions (the patient rests). An acoustic field should then be picked up in a restricted circular zone at the body surface opposite the diseased segment of vessel (as follows from the variation of the spectrum E_{ob} with vertical distance from a stenosis shown in Figure 6). The further (vertically) we are from that place, the lower our chances of finding a stenosis.

In the study of the hydrodynamics of a stenosis, the concept of the "critical" stenosis is used, with the critical stenosis, S_{cr}, generally defined as one for which a small further reduction in lumen area will cause significant changes in the characteristics of the hydrodynamic field. Typically [3, 4], it is found that the values for S_{cr} vary widely (50–90%) depending on the conditions of the patient. In this experiment, we were able to detect milder stenoses for which $S \approx 20\%$. This may be a reason for introducing the "critical" stenosis in

the study of acoustic diagnosis techniques, and might therefore stimulate researchers into finding the relationships between S_{cr} and the parameters of stenosis, vessel and flow.

6. CONCLUSIONS

The results obtained in the experiment and their analysis allow us to draw the following conclusions:

1. A vascular stenosis has *two basic* acoustic effects. These are a general increase in the radiated sound level and the production of a number of additional distinct peaks (the new frequency components) in the acoustic power spectrum.
2. The difference between the levels of noise from stenosed and intact pipes increases/decreases as the stenosis severity and(or) the flow Reynolds number increases/decreases (see estimate (20)); this difference decreases/increases as the stenosis length increases/decreases.
3. The frequencies of the additional peaks are close to the characteristic frequencies of vortex formation in the disturbed flow region behind a stenosis (formulas (10), (11) and (13)) and the resonance frequencies of vibration of the post-stenotic segment of pipe.
4. The stenosis-generated acoustic power is approximately proportional to the fourth power of the stenosis severity and the fourth power of the flow Reynolds number (formulas (7) and (19)).

ACKNOWLEDGMENTS

The author gratefully acknowledges the financial support of the Alexander von Humboldt Foundation (Germany) and useful comments given by Prof. V. Grinchenko and Prof. P. Költzsch in discussing this work. Thanks are also expressed to Jü.Landgraf, A. Witing and A. Wilde for their help in developing the experimental system.

REFERENCES

1. L. H. Back and E. J. Roschke 1972 *Transactions of the American Society of Mechanical Engineers, Journal of Applied Mechanics, Series E* **39**, 677–681. Shear-layer flow regimes and wave instabilities and reattachment lengths downstream of an abrupt circular channel expansion.
2. R. A. Cassanova and D. P. Giddens 1978 *Journal of Biomechanics* **11**, 441–453. Disorder distal to modeled stenoses in steady and pulsatic flows.
3. D. F. Young 1979 *Journal of Biomechanical Engineering* **101**, 157–175. Fluid mechanics of arterial stenoses.
4. S. G. Mirolyubov 1983 *Modern Problems in Biomechanics* **1**, 73–136. Hydrodynamics of stenosis (in Russian).
5. C. Clark 1976 *Journal of Biomechanics* **9**, 521–528. The fluid mechanics of aortic stenosis. 1. Theory and steady flow experiments.
6. C. Clark 1977 *Journal of Biomechanics* **10**, 461–472. Turbulent wall pressure measurements in a model of aortic stenosis.
7. R. J. Tobin and I. D. Chang 1976 *Journal of Biomechanics* **9**, 633–640. Wall pressure spectra scaling downstream of stenoses in steady tube flow.
8. S. C. Crow and F. H. Champagne 1971 *Journal of Fluid Mechanics* **48**, 547–591. Orderly structure in jet turbulence.
9. G. Pedrizzetti 1996 *Journal of Fluid Mechanics* **310**, 89–111. Unsteady tube flow over an expansion.
10. S. A. Abdallah and N. H. C. Hwang 1988 *Journal of the Acoustical Society of America* **83**, 318–334. Arterial stenosis murmurs: an analysis of flow and pressure fields.

11. J. J. FREDBERG 1974 *Bulletin of Mathematical Biology* **36**, 143–155. Pseudo-sound generation at atherosclerotic constrictions in arteries.
12. J. J. FREDBERG 1977 *Journal of the Acoustical Society of America* **61**, 1077–1085. Origin and character of vascular murmurs: model studies.
13. B. KIM and W. K. CORCORAN 1974 *Journal of Biomechanics* **7**, 335–342. Experimental measurement of turbulence spectra distal to stenosis.
14. R. L. KIRKEEIDE, D. F. YOUNG and N. R. CHOLVIN 1977 *Journal of Biomechanics* **10**, 431–441. Wall vibrations induced by flow through simulated stenoses in models and arteries.
15. D. P. GIDDENS, R. F. MABON and R. A. CASSANOVA 1976 *Circulation Research* **39**, 112–119. Measurements of disordered flow distal to subtotal vascular stenosis in the thoracic aortas of canines.
16. A. A. BORISYUK 2000 *Acoustic Bulletin* **3**(2), 3–18. Modeling of noise generation by a vascular stenosis (in Russian).
17. A. O. BORISYUK 1993 *Ph. D. Thesis, Institute of Hydromechanics, Kiev, Ukraine*. Vibration and sound radiation by elastic plates excited by turbulent flow (in Russian).
18. A. O. BORISYUK and V. T. GRINCHENKO 1997 *Journal of Sound and Vibration* **204**, 213–237. Vibration and noise generation by elastic elements excited by a turbulent flow.
19. W. K. BLAKE 1986 *Mechanics of Flow-Induced Sound and Vibration*, 2 Vols. New York: Academic Press.
20. I. V. VOVK, K. E. ZALUTSKII and L. G. KRASNYI 1994 *Akysticheskii zhurnal* **40**, 762–767. Acoustic model of the human respiratory system (in Russian).
21. I. V. VOVK, V. T. GRINCHENKO and V. N. OLEINIK 1995 *Acoustical Physics* **41**, 667–676. Modeling the acoustic properties of the chest and measuring breath sounds.
22. J. WANG, B. TIE, W. WELKOWITZ, J. L. SEMMLOW and J. B. KOSTIS 1990 *IEEE Transactions of Biomedical Engineering* **37**, 1087–1094. Modeling sound generation in stenosed coronary arteries.
23. A. O. BORISYUK 1998 *Acoustic Bulletin* **1**(3), 3–13. Modeling of the acoustic properties of a larger human blood vessel.
24. A. O. BORISYUK 1999 *Flow, Turbulence and Combustion* **61**, 269–284. Noise field in the human chest due to turbulent flow in a larger blood vessel.
25. J. C. LAU, J. J. FISHER and H. V. FUCHS 1972 *Journal of Sound and Vibration* **22**, 379–406. The intrinsic structure of turbulent jets.
26. J. C. LAU 1979 *Proceedings of the Royal Society of London Series A* **368**, 547–571. The vortex street structure of turbulent jets, Part2.
27. A. O. BORISYUK 2001 *Reports of the National Academy of Sciences of Ukraine* **6**, 47–51. Modelling of the acoustic field of blood vessel in presence of wall thickening (in Ukrainian).
28. H. SCHLICHTING 1960 *Boundary Layer Theory*. New York: McGraw-Hill, third edition.

APPENDIX A: NOMENCLATURE

D	inner diameter of pipe
h	wall thickness of pipe
A_0	cross-sectional area of pipe
a	midsurface radius of pipe
E_v	modulus of elasticity of pipe wall
ρ_v	mass density of pipe wall
v_v	The Poisson's ratio of pipe wall
c_v	longitudinal wave speed in pipe wall
d	inner diameter of a stenosis
l	length of a stenosis
A	cross-sectional area of a stenosis
S	stenosis severity
R	cross-sectional radius of test section
H	water level in test section
γ_m, α_m	wavenumbers of test volume
k_0	acoustic wavenumber in test volume
c_0	sound speed in test volume
ρ_0	mass density of acoustic medium in test volume
L_j	length of the jth segment of a stenosed pipe ($j = \mathrm{I}, \mathrm{II}$)

$f_{n*}^{(j)}$ resonance frequencies of the jth segment of a stenosed pipe
$k_n^{(j)}$ modal wavenumbers of the jth segment of a stenosed pipe
$m_n^{(j)}$ modal added masses of the jth segment of a stenosed pipe
$Z_n^{(j)}$ modal radiation impedances of the jth segment of a stenosed pipe
(r, ϕ, z) cylindrical co-ordinates
f frequency
$f_{ch}^{(r)}$ characteristic frequencies ($r = 1, \ldots, 4$)
T period of acquisition of analyzer
Q water volume flowing in collection tank during period T
U mean axial flow velocity in pipe
u mean axial flow velocity in the stenosis region
u_c convective velocity
v kinematic viscosity
Re_D flow Reynolds number
Re_{cr} critical Reynolds number
P, P_i wall pressure power spectra ($i = 1, 3, 4, 5$)
E_j acoustic power spectrum of the jth segment of a stenosed pipe
E_{ob} acoustic power spectrum of a stenosed pipe
E_{nor} acoustic power spectrum of a normal pipe
ζ relative deflection coefficient